## ChemComm

### COMMUNICATION

Check for updates

Cite this: Chem. Commun., 2020, 56, 9449

Received 11th May 2020, Accepted 10th July 2020

DOI: 10.1039/d0cc03385e

rsc.li/chemcomm



View Article Online View Journal | View Issue

# Nucleophilic reactivity of a mononuclear cobalt(III)-bis(tert-butylperoxo) complex<sup>†</sup>

Bongki Shin, () + Younwoo Park, + Donghyun Jeong and Jaeheung Cho +

A mononuclear cobalt(III)-bis(tert-butylperoxo) adduct  $(Co^{III}-(OO^tBu)_2)$  bearing a tetraazamacrocyclic ligand was synthesized and characterized using various physicochemical methods, such as X-ray, UV-vis, ESI-MS, EPR, and NMR analyses. The crystal structure of the  $Co^{III}-(OO^tBu)_2$  complex clearly showed that two OO<sup>t</sup>Bu ligands bound to the equatorial position of the cobalt(III) center. Kinetic studies and product analyses indicate that the  $Co^{III}-(OO^tBu)_2$  intermediate exhibits nucleophilic oxidative reactivity toward external organic substrates.

Transition metal–alkylperoxo (M–OOR) species play an important role in oxidation reactions such as industrial and biological catalytic oxidation.<sup>1–6</sup> In industrial processes, M–OOR intermediates, such as Co<sup>III</sup>–OOR complexes, were proposed as key intermediates in hydrocarbon catalytic oxidation under harsh conditions.<sup>1,7</sup> Mononuclear nonheme M–OOR complexes have been suggested to play a significant role in the oxidation reaction of metalloenzyme systems (*e.g.*, lipoxygenase and homoprotocatechuate 2,3-dioxygenase).<sup>8,9</sup> Biomimetic studies of M–OOR complexes enabled catalysts to be developed that produce high value-added organic products under mild conditions.

Mononuclear heme and nonheme first-row M–OOR intermediates (M = Mn, Fe, Co, Ni, and Cu) have been investigated as model complexes for the active sites of metalloenzymes.<sup>2,5,6,10–13</sup> A number of M–OOR complexes were mainly studied in the investigation of electrophilic reactions (*e.g.*, oxygen and hydrogen atom transfer reaction).<sup>14–25</sup> It has been reported that the reaction proceeds *via* the •OOR and •OR radicals from decomposition of the M–OOR species.<sup>1</sup> However, only a few examples of nucleophilic reactivity with M–OOR intermediates (M = Fe, Ni, and Cu) have been reported.<sup>19,20,23</sup>

In the Sharpless-Katsuki epoxidation,  $Ti-(OOR)_n$  (n = 1-4)species were proposed as reactive intermediates.<sup>26,27</sup> Furthermore, in the formation of Fe–OO<sup>t</sup>Bu complexes,  $Fe-(OO^tBu)_2$  species,  $[Fe^{III}(TPP)(OO^tBu)_2]^-$  (TPP = 5,10,15,20-tetraphenylporphyrinate) and  $[Fe^{III}(BPMCN)(OO^{t}Bu)(HOO^{t}Bu)]^{2+}$  (BPMCN = N,N'-bis (2-pyridylmethyl-*N*,*N*'-dimethyl-*trans*-1,2-diaminocyclohexane)) adducts, have been proposed as short-lived intermediates.<sup>28-31</sup> However, definitive evidence of bis(alkylperoxo) binding firstrow transition metal compounds has not been reported yet. In this work, we report a fully characterized  $Co^{III}$ -(OO<sup>t</sup>Bu)<sub>2</sub> complex bearing a tetraazamacrocyclic ligand, [Co<sup>III</sup>(Me<sub>3</sub>-TPADP)(OO<sup>t</sup>Bu)<sub>2</sub>]<sup>+</sup> (2, Me<sub>3</sub>-TPADP = 3,6,9-trimethyl-3,6,9-triaza-1 (2,6)-pyridinacyclodecaphane). Intermediate 2 was investigated in nucleophilic reactions such as aldehyde oxidation. Only one of the two OO<sup>t</sup>Bu ligands in 2 is able to oxidize external substrates. In order to compare the structure and the reactivity of an alkylperoxo and bis(alkylperoxo) binding cobalt species, Co<sup>III</sup>- $(OO^{t}Bu)(X)$  complexes,  $[CO^{III}(Me_{3}-TPADP)(OO^{t}Bu)(X)]^{+}$   $(X = N_{3})$ for 4, NCS for 5), were prepared as well.

The cobalt(II) starting complex,  $[Co^{II}(Me_3-TPADP)(CH_3CN)_2]^{2+}$ (1), was synthesized by using a published method.<sup>32</sup> When 10 equiv. of *tert*-butyl hydroperoxide (<sup>*t*</sup>BuOOH) was added to 1 in the presence of 2 equiv. of triethylamine (TEA) in CH<sub>3</sub>CN at 25 °C, the Co<sup>III</sup>–(OO<sup>*t*</sup>Bu)<sub>2</sub> adduct,  $[Co^{III}(Me_3-TPADP)(OO<sup>$ *t* $</sup>Bu)_2]^+$ (2), was generated and the solution color changed from purple to dark green (Scheme S1, ESI†). Intermediate 2 is thermally metastable in CH<sub>3</sub>CN at 25 °C, which allowed us to use it for characterization and reactivity studies.

The UV-vis spectrum of 2 in CH<sub>3</sub>CN at 25 °C shows electronic absorption bands at  $\lambda_{max} = \sim 360$  ( $\varepsilon = 1100 \text{ M}^{-1} \text{ cm}^{-1}$ ) and 583 nm ( $\varepsilon = 190 \text{ M}^{-1} \text{ cm}^{-1}$ ) (Fig. 1a). Electrospray ionization mass spectrometry (ESI-MS) analysis of 2 exhibits a prominent ion peak at m/z 485.3, whose mass and isotope distribution pattern correspond to [Co<sup>III</sup>(Me<sub>3</sub>-TPADP)(OO<sup>t</sup>Bu)<sub>2</sub>]<sup>+</sup> (calcd m/z485.3) (Fig. 1b). The X-band electron paramagnetic resonance (EPR) silence (Fig. 1a, inset) and <sup>1</sup>H NMR spectral features (Fig. S1, ESI<sup>+</sup>) in the diamagnetic region confirm that complex 2 is a low-spin S = 0 cobalt(m) species.

Department of Emerging Materials Science, DGIST, Daegu 42988, Korea. E-mail: jaeheung@dgist.ar.kr

<sup>&</sup>lt;sup>†</sup> Electronic supplementary information (ESI) available: Synthesis and characterization data and kinetic details. CCDC 1906994–1906996. For ESI and crystallographic data in CIF or other electronic format see DOI: 10.1039/ d0cc03385e

<sup>‡</sup> These authors contributed equally to this work.

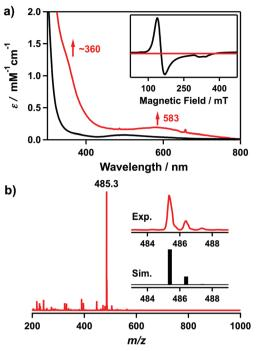


**Fig. 1** (a) UV-vis spectra of  $[Co^{II}(Me_3-TPADP)(CH_3CN)_2]^{2+}$  (1) (the black line) and  $[Co^{III}(Me_3-TPADP)(OO^{T}Bu)_2]^{+}$  (2) (the red line) in CH<sub>3</sub>CN at 25 °C.<sup>32</sup> Inset shows the X-band EPR spectra of 1 (the black line) in frozen CH<sub>3</sub>CN at 5 K and 2 (the red line) in frozen CH<sub>3</sub>CN at 113 K.<sup>32</sup> The parameters for the measurement of 2: microwave power = 1.0 mW, frequency = 9.176 GHz, sweep width = 0.40 T, and modulation amplitude = 0.60 mT. (b) ESI-MS of 2 in CH<sub>3</sub>CN at -40 °C. Insets show experimental (upper) and simulated (lower) isotope distribution patterns.

The X-ray crystal structure of  $[Co^{III}(Me_3-TPADP)(OO'Bu)_2]$ (BPh<sub>4</sub>)(Et<sub>2</sub>O) (2-BPh<sub>4</sub>·Et<sub>2</sub>O) revealed a distorted octahedral geometry where two *tert*-butyl peroxide ligands coordinate to the cobalt(III) center in the *cis* positions (Fig. 2a). To the best of our knowledge, this is the first crystal structure of a mononuclear Co<sup>III</sup>–(OO<sup>t</sup>Bu)<sub>2</sub> complex. The average Co–O (1.8590 Å) and O–O (1.4757 Å) bond distances of **2** are comparable to those of the Co<sup>III</sup>–OO<sup>t</sup>Bu complexes (Table S2, ESI<sup>†</sup>).<sup>1,33</sup>

Thermal decomposition of 2 produced a Co<sup>III</sup>-(OO<sup>t</sup>Bu)(OH) complex,  $[Co^{III}(Me_3-TPADP)(OO^tBu)(OH)]^+$  (3), in  $CH_3CN$ at 25 °C (Fig. S2, ESI<sup>†</sup>).<sup>34</sup> Formation of 3 was confirmed by cold spray ionization spectrometry (CSI-MS). The CSI-MS spectrum of 3 shows a prominent signal at m/z 413.17 (calcd m/z413.20) (Fig. S3, ESI<sup> $\dagger$ </sup>). Upon adding isotopically labeled H<sub>2</sub><sup>18</sup>O and D<sub>2</sub>O into the solution of 3, mass peaks at 415.21 and 414.22 corresponding to [Co<sup>III</sup>(Me<sub>3</sub>-TPADP)(OO<sup>t</sup>Bu)(<sup>18</sup>OH)]<sup>+</sup> (calcd m/z 415.20) and  $[Co^{III}(Me_3-TPADP)(OO^tBu)(OD)]^+$ (calcd m/z 414.20), respectively, were observed (Fig. S3, ESI,<sup>†</sup> the inset). These mass shifts demonstrate that 3 contains a hydroxide ligand. In a previous study, the  $Fe-(OO^tBu)_2$  species was also proposed as a precursor of the Fe-(OO<sup>t</sup>Bu) species.<sup>29</sup> Tajima *et al.* insisted that  $[Fe^{III}(TPP)(OO^tBu)_2]^-$ , generated by adding an excess amount of sodium methoxide (NaOCH<sub>3</sub>) and <sup>t</sup>BuOOH to the [Fe<sup>III</sup>(TPP)]<sup>+</sup> solution, reacted with additional NaOCH<sub>3</sub>, affording the formation of the  $[Fe^{III}(TPP)(OO^tBu)]$ (OCH<sub>3</sub>)]<sup>-</sup> species.<sup>29</sup>

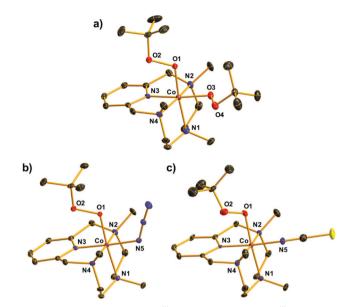
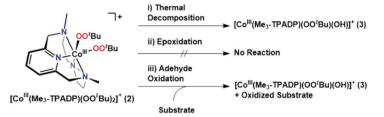


Fig. 2 ORTEP plots of the (a)  $Co^{III}$ -(OO<sup>t</sup>Bu)<sub>2</sub> complex, [Co<sup>III</sup>(Me<sub>3</sub>-TPADP) (OO<sup>t</sup>Bu)<sub>2</sub>]<sup>+</sup> (**2**), and Co<sup>III</sup>-(OO<sup>t</sup>Bu)(X) complexes, [Co<sup>III</sup>(Me<sub>3</sub>-TPADP) (OO<sup>t</sup>Bu)(X)]<sup>+</sup> (X = (b) N<sub>3</sub> (**4**), (c) NCS (**5**)), with thermal ellipsoids drawn at the 30% probability level. Hydrogen atoms are omitted for clarity.

We then investigated the electrophilic and nucleophilic reactivities of 2. The electrophilic reaction of 2 was performed by using styrene and 2,3-dimethyl-2-butene. Upon addition of substrates to the solution of 2 in CH<sub>3</sub>CN at 10 °C, the intermediate remained intact without showing specific UV-vis spectral changes, and product analysis of these reaction solutions did not show oxidized products (Scheme 1). In contrast, the nucleophilic reactivity of 2 was observed in the oxidation of aldehydes (Scheme 1). Upon the addition of benzaldehyde to 2 in CH<sub>3</sub>CN at 15 °C, the characteristic absorption band of 2 disappeared with a pseudo-first-order decay (Fig. 3a, the inset and Table S3, ESI<sup>†</sup>). The product analysis of the reaction solution revealed that benzoic acid (95(1)%) was produced in the oxidation of benzaldehyde (Scheme S2, ESI<sup>+</sup>). In addition, the cobalt(II)-benzoato complex,  $[Co^{II}(Me_3-TPADP)(C_6H_5COO)]^+$ , was generated after the reaction was completed (Fig. S7, ESI<sup>+</sup> for CSI-MS analysis). The reactivity of 2 was further investigated with para-substituted benzaldehydes, para-X-Ph-CHO (X = Me, F, Cl, and CF<sub>3</sub>) (Table S3, ESI<sup>†</sup>). The Hammett plot of the pseudofirst-order rate constants versus  $\sigma_p^+$  gave a  $\rho$  value of 0.7(1) (Fig. 3b). The positive  $\rho$  value indicates that 2 has nucleophilic character. The reactivity of 2 was further examined by using primary (1-pentanal for 1°-CHO), secondary (2-methylbutanal for 2°-CHO), and tertiary (pivalaldehyde for 3°-CHO) aldehydes, and the observed reactivity order of  $1^{\circ}$ -CHO >  $2^{\circ}$ -CHO >  $3^{\circ}$ -CHO supports the nucleophilic character of 2 as well (Fig. S8, ESI<sup>+</sup>). Product analyses of the resulting solutions revealed that pentanoic acid (94(3)%), 2-methylbutanoic acid (94(4)%), and 2,2dimethylpropanoic acid (94(1)%) were produced in the oxidation of 1-pentanal, 2-methylbutanal, and pivalaldehyde, respectively (Table S4, ESI<sup>†</sup>).

Upon the addition of 2-phenyl propional dehyde (2-PPA) to 2 in CH<sub>3</sub>CN at 25  $^\circ \rm C$  under a erobic conditions, the UV-vis absorption



Scheme 1 Overall electrophilic and nucleophilic reactivities of 2, 4 and 5.

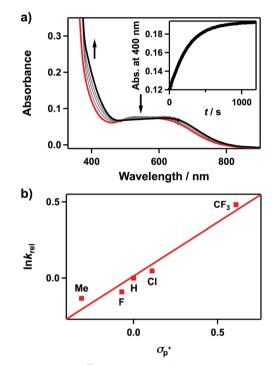
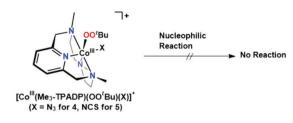


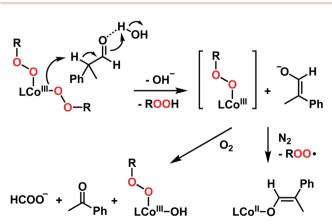
**Fig. 3** Reactions of  $[Co^{III}(Me_3-TPADP)(OO^{t}Bu)_2]^+$  (**2**) with benzaldehyde in CH<sub>3</sub>CN/MeOH (v/v = 3 : 1). (a) UV-vis spectral changes of **2** (0.5 mM) upon addition of 200 equiv. of benzaldehyde at 15 °C. Inset shows the time course of the absorbance at 400 nm. (b) Hammett plot of ln  $k_{rel}$  against  $\sigma_p^+$  of *para*-substituted benzaldehydes. The  $k_{rel}$  values were calculated by dividing  $k_{obs}$  of *para*-X-Ph-CHO (X = Me, F, H, Cl, and CF<sub>3</sub>) by  $k_{obs}$  of benzaldehyde at 15 °C.

band of 2 slightly changed with isosbestic points at 390 and 452 nm, which follows a pseudo-first-order decay profile (Fig. S9, ESI<sup>†</sup>). The pseudo-first-order rate constants increased proportionally with the 2-PPA concentration, giving a second-order rate constant  $(k_2)$  of 4.1(3) × 10<sup>-1</sup> M<sup>-1</sup> s<sup>-1</sup> at 25 °C (Fig. S10a, ESI†). After the reaction of 2 with 2-PPA, product analysis revealed that acetophenone (95(1)%) was produced as a final product. The CSI-MS spectrum of the reaction solution revealed the formation of 3 and a small amount of cobalt(II)-formato species was also detected under an inert atmosphere (Fig. S11, ESI<sup>+</sup>). The temperature dependence of the  $k_2$  values was examined in the range of 273-298 K, where a linear Eyring plot was obtained with the activation parameters of  $\Delta H^{\ddagger} = 11(1)$  kcal mol<sup>-1</sup> and  $\Delta S^{\ddagger} =$ -22(3) cal mol<sup>-1</sup> K<sup>-1</sup> (Fig. S10b, ESI<sup>†</sup>). The observed negative entropy value and the second-order kinetics suggest that the oxidation of 2-PPA by 2 is performed through a bimolecular mechanism.



Interestingly, the same reaction performed under a  $N_2$ atmosphere gives different products. The reaction of 2 with 2-PPA under N<sub>2</sub> in CH<sub>3</sub>CN at 25 °C gave a new absorption band at 480 nm (Fig. S12, ESI<sup>+</sup>). By analysing the resulting solution with CSI-MS, we found that a  $cobalt(\pi)$ -enolate complex, [Co<sup>II</sup>(Me<sub>3</sub>-TPADP)(OCH=C(Me)Ph)]<sup>+</sup>, was formed as a decomposed product (Fig. S13, ESI<sup>†</sup>). The product analysis of the reaction solution indicated that trace amounts of acetophenone were produced (<1%) after the reaction. When the cobalt(II)enolate complex was exposed to  $O_2$ , a cobalt( $\pi$ )-formato complex was obtained as a major product, as observed by CSI-MS (Fig. S14, ESI†). These results are very similar to Tolman's recent mechanism of the aldehyde deformylation pathway via a copper(II)enolate species.35 Based on the kinetic studies and product analyses under N<sub>2</sub> and O<sub>2</sub>, the possible reaction mechanisms for 2-PPA oxidation by 2 are summarized in Scheme 2. The reaction of 2 and 2-PPA in the presence of water afforded enolate and a putative cobalt( $\mu$ )–(OO<sup>t</sup>Bu) species through  $\alpha$ -deprotonation of 2-PPA by one of the alkylperoxides of 2. The putative cobalt(m)-(OO<sup>t</sup>Bu) species decomposed to the cobalt(II)-enolate complex under  $N_2$ . In the presence of  $O_2$ , the enolate is oxidized to acetophenone, and complex 3 is produced as a final product.

In the aldehyde oxidation, only one OO<sup>t</sup>Bu ligand in 2 was able to participate in the oxidation of 2-PPA (Scheme 1). To compare the reactivity properties of  $\text{Co}^{\text{III}}$ -( $\text{OO}^{t}\text{Bu}$ ) and  $\text{Co}^{\text{III}}$ -( $\text{OO}^{t}\text{Bu}$ )<sub>2</sub> complexes,  $\text{Co}^{\text{III}}$ -( $\text{OO}^{t}\text{Bu}$ )(X) complexes,  $[\text{Co}^{\text{III}}(\text{Me}_{3}-\text{TPADP})(\text{OO}^{t}\text{Bu})(\text{X})]^{+}$  (X = N<sub>3</sub> for 4, NCS for 5), were synthesized. 4 and 5 were prepared by adding 1.1 equiv. of NaX (X = N<sub>3</sub>, NCS) to the reaction solution of **1** in CH<sub>3</sub>CN at 25 °C and then 5 equiv.



Scheme 2 Proposed reaction pathways of 2 with 2-PPA under N\_2 and O\_2 (L = Me\_3-TPADP, R =  ${}^tBu$ ).

of <sup>t</sup>BuOOH and 2 equiv. of TEA were added (Scheme S1, ESI†). Characterization of 4 and 5 was performed by UV-vis, ESI-MS, EPR, and <sup>1</sup>H NMR analyses (Experimental section and Fig. S15–S19, ESI†).

The single crystals of **4** and **5** revealed a similar distorted octahedral geometry to that of **2** in which one OO<sup>*t*</sup>Bu ligand bound to the cobalt(m) center was located in the *trans* position of the amine group and the other anionic monodentate ligand, X, was located in the *trans* position of the pyridine ring (Fig. 2b and c). These data clearly indicate that the OO<sup>*t*</sup>Bu ligand in the *trans* position of the pyridine ring in **2** was substituted with an anionic ligand in **3** and **4**. The Co–O1 bond distances (1.862(3) Å for **4**, 1.880(4) Å for **5**) and O1–O2 bond distances (1.479(4) Å for **4**, 1.430(6) Å for **5**) were within the range of those of the reported Co<sup>III</sup>–OO<sup>*t*</sup>Bu complexes and similar to those of **2** (Table S2, ESI<sup>†</sup>).<sup>1,33</sup>

In the reactions of 4 and 5 with 2-PPA, we could not observe any change in the UV-vis spectra. Based on the reactivity and structural comparison of 2, 4, and 5, the reaction site of 2 is presumed to be the  $OO^tBu$  ligand in the *trans* position of the pyridine ring. Further theoretical calculations on the detailed reaction mechanism of 2 with substrates are underway and will clarify the reaction site of 2.

In conclusion, we have synthesized and characterized a mononuclear  $\text{Co}^{\text{III}}$ – $(\text{OO}^{t}\text{Bu})_2$  intermediate,  $[\text{Co}^{\text{III}}(\text{Me}_3\text{-TPADP})$  $(\text{OO}^{t}\text{Bu})_2]^+$  (2), with various physicochemical methods including UV-vis, ESI-MS, EPR, X-ray, and NMR analyses. In the kinetic studies, under mild conditions, one of the two OO'Bu ligands in 2 is capable of performing a nucleophilic reaction (*i.e.*, aldehyde oxidation). A Co<sup>III</sup>– $(\text{OO}^{t}\text{Bu})(\text{OH})$  complex, 3, was generated by thermal decomposition of 2 and/or deformylation reaction of 2-PPA by 2 in the presence of O<sub>2</sub>. Furthermore, Co<sup>III</sup>– $(\text{OO}^{t}\text{Bu})$  complexes,  $[\text{Co}^{\text{III}}(\text{Me}_3\text{-TPADP})(\text{OO}^{t}\text{Bu})(\text{X})]^+$  (X = N<sub>3</sub> for 4, NCS for 5), which have a OO'Bu ligand in the *trans* position of the amine group were prepared, and 4 and 5 did not undergo aldehyde oxidation.

This research was supported by the NRF (2019R1A2C2086249 and 2018R1A5A1025511) and the Ministry of Science, ICT and Future Planning (CGRC 2016M3D3A01913243) of Korea.

### Conflicts of interest

The authors declare no competing financial interest.

#### Notes and references

- 1 F. A. Chavez and P. K. Mascharak, Acc. Chem. Res., 2000, 33, 539-545.
- 2 S. Hikichi, M. Akita and Y. Moro-Oka, *Coord. Chem. Rev.*, 2000, **198**, 61–87.
- 3 M. Costas, M. P. Mehn, M. P. Jensen and L. Que, Jr., *Chem. Rev.*, 2004, **104**, 939–986.

- 4 B. de Bruin, P. H. M. Budzelaar and A. W. Gal, *Angew. Chem., Int. Ed.*, 2004, **43**, 4142–4157.
- 5 S. Itoh, Acc. Chem. Res., 2015, 48, 2066-2074.
- 6 A. T. Fiedler and A. A. Fischer, J. Biol. Inorg. Chem., 2017, 22, 407-424.
- 7 J. F. Black, J. Am. Chem. Soc., 1978, 100, 527–535.
- 8 E. G. Kovaleva and J. D. Lipscomb, Science, 2007, 316, 453-457.
- 9 E. Skrzypczak-Jankun, R. A. Bross, R. T. Carroll, W. R. Dunham and M. O. Funk, Jr., *J. Am. Chem. Soc.*, 2001, **123**, 10814–10820.
- 10 H. Komatsusuzaki, N. Sakamoto, M. Satoh, S. Hikichi, M. Akita and Y. Moro-oka, *Inorg. Chem.*, 1998, **37**, 6554–6555.
- 11 S. Hong, Y.-M. Lee, K.-B. Cho, M. S. Seo, D. Song, J. Yoon, R. Garcia-Serres, M. Clémancey, T. Ogura, W. Shin, J.-M. Latour and W. Nam, *Chem. Sci.*, 2014, 5, 156–162.
- 12 J. A. Kovac, Acc. Chem. Res., 2015, 48, 2744-2753.
- 13 M. Sankaralingam, Y.-M. Lee, W. Nam and S. Fukuzumi, *Coord. Chem. Rev.*, 2018, **365**, 41–59.
- 14 N. Kitajima, T. Katayama, K. Fujisawa, Y. Iwata and Y. Morooka, J. Am. Chem. Soc., 1993, 115, 7872–7873.
- 15 J. Kim, E. Larka, E. C. Wilkinson and L. Que, Jr., Angew. Chem., Int. Ed. Engl., 1995, 34, 2048–2051.
- 16 M. S. Seo, T. Kamachi, T. Kouno, K. Murata, M. J. Park, K. Yoshiza-wa and W. Nam, *Angew. Chem., Int. Ed.*, 2007, **46**, 2291–2294.
- 17 S. Gosiewska, H. P. Permentier, A. P. Bruins, G. van Koten and R. J. M. Gebbink, *Dalton Trans.*, 2007, 3365–3368.
- 18 A. Kunishita, H. Ishimaru, S. Nakashima, T. Ogura and S. Itoh, J. Am. Chem. Soc., 2008, 130, 4244–4245.
- 19 S. Hikichi, H. Okuda, Y. Ohzu and M. Akita, *Angew. Chem., Int. Ed.*, 2009, **48**, 188–191.
- 20 J. Stasser, F. Namuswe, G. D. Kasper, Y. Jiang, C. M. Krest, M. T. Green, J. Penner-Hahn and D. P. Goldberg, *Inorg. Chem.*, 2010, **49**, 9178–9190.
- 21 T. Tano, M. Z. Ertem, S. Yamaguchi, A. Kunishita, H. Sugimoto, N. Fujieda, T. Ogura, C. J. Cramer and S. Itoh, *Dalton Trans.*, 2011, 40, 10326–10336.
- 22 S. Paria, T. Ohta, Y. Morimoto, T. Ogura, H. Sugimoto, N. Fujieda, K. Goto, K. Asano, T. Suzuki and S. Itoh, *J. Am. Chem. Soc.*, 2015, 137, 10870–10873.
- 23 B. Kim, D. Jeong and J. Cho, Chem. Commun., 2017, 53, 9328-9331.
- 24 T. Abe, Y. Morimoto, K. Mieda, H. Sugimoto, N. Fujieda, T. Ogura and S. Itoh, *J. Inorg. Biochem.*, 2017, **177**, 375–383.
- 25 J. Lewiński, Z. Ochal, E. Bojarski, E. Tratkiewicz, I. Justyniak and J. Lipkowski, *Angew. Chem., Int. Ed.*, 2003, **42**, 4643–4646.
- 26 T. Katsuki and K. B. Sharpless, J. Am. Chem. Soc., 1980, 102, 5974–5976.
- 27 D. E. Babushkin and E. P. Talsi, J. Mol. Catal. A: Chem., 2003, 200, 165–175.
- 28 M. Rivera, G. A. Caignan, A. V. Astashkin, A. M. Raitsimring, T. K. Shokhireva and F. A. Walker, *J. Am. Chem. Soc.*, 2002, **124**, 6077–6089.
- 29 K. Tajima, K. Tada, J. Jinno, T. Edo, H. Mano, N. Azuma and K. Makino, *Inorg. Chim. Acta*, 1997, **254**, 29–35.
- 30 M. P. Jensen, M. Costas, R. Y. N. Ho, J. Kaizer, A. Mairata i Payeras, E. Münck, L. Que, Jr., J.-U. Rohde and A. Stubna, *J. Am. Chem. Soc.*, 2005, **127**, 10512–10525.
- 31 M. P. Jensen, A. M. I. Payeras, A. T. Fiedler, M. Costas, J. Kaizer, A. Stubna, E. Münck and L. Que, Jr., *Inorg. Chem.*, 2007, 46, 2398–2408.
- 32 B. Shin, K. D. Sutherlin, T. Ohta, T. Ogura, E. I. Solomon and J. Cho, *Inorg. Chem.*, 2016, 55, 12391–12399.
- 33 F. A. Chavez, C. V. Nguyen, M. M. Olmstead and P. K. Mascharak, *Inorg. Chem.*, 1996, 35, 6282–6291.
- 34 Interestingly, the decay of 2 was facilitated by adding excess water in 2, and a cobalt(n)-hydroxo complex was observed as a major peak in CSI-MS (Fig. S4–S6, ESI†).
- 35 W. D. Bailey, N. L. Gagnon, C. E. Elwell, A. C. Cramblitt, C. J. Bouchey and W. B. Tolman, *Inorg. Chem.*, 2019, 58, 4706–4711.